

EFFECTS OF TREPROSTINIL SODIUM IN A MONOCROTALINE-INDUCED RAT  
MODEL OF PULMONARY HYPERTENSION

---

A Thesis presented to the Faculty of the Graduate School  
University of Missouri-Columbia

---

In Partial Fulfillment  
of the Requirements for the Degree

Master of Science

---

by  
SHENA L. LATCHAM

Dr. Jeffrey W. Skimming and Dr. Vincent G. DeMarco, Thesis Supervisors

MAY 2005

The undersigned, appointed by the Dean of the Graduate School,  
have examined the thesis entitled.

EFFECTS OF TREPROSTINIL IN SODIUM IN A MONOCROTALINE-INDUCED  
RAT MODEL OF PULMONARY HYPERTENSION

Presented by Shena Latcham

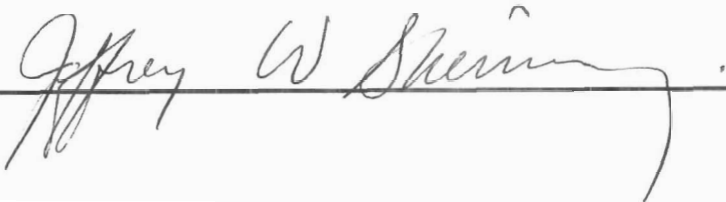
A candidate for the degree of Master of Physiology

And hereby certify that in their opinion it is worthy of acceptance.

  
\_\_\_\_\_

  
\_\_\_\_\_

  
\_\_\_\_\_

  
\_\_\_\_\_

## ACKNOWLEDGEMENTS

I would like to extend my gratitude to Dr. Jeffrey Skimming and Dr. Vincent DeMarco for their guidance and assistance in helping me to develop, carry-out, and complete this thesis project. Their knowledge and expertise in the field of pulmonary hypertension, as well as their patience and encouragement served as a great asset whenever I needed assistance at any stage of the experimental process. Also, I greatly appreciate the suggestions and time given by Dr. Michael Rovetto and Dr. Kerry McDonald, members of my thesis committee. Also, thank you to Tammy Strawn, Jim Bosanquet, Vinay Rawlani, and Karen Bauer, the other members of the Skimming/DeMarco laboratory. Working as a team, we helped each other learn experimental techniques, collect data, and interpret results, in addition to making the lab a fun learning environment that was always full of excitement. Finally, I would like to thank Dr. James Turk for his insight and for the use of his microscope equipment and software.

I would also like to dedicate this thesis to my parents, Ronald Latcham, Dixie Latcham and Sandy Dew, and my sisters, Alison Latcham and Michelle Dew, as well as my first mentor, Dr. Betty Herndon, for always supporting and encouraging my love of science. Most of all, I would like dedicate this work to my husband, Matthew Sparks, who helped me complete this project by teaching me patience and making it easier to get through those long days and late nights in the lab.

## TABLE OF CONTENTS

ACKNOWLEDGEMENTS.....	ii
LIST OF ILLUSTRATIONS.....	iv
LIST OF ABBREVIATIONS.....	v
ABSTRACT.....	vi
Chapter	
I. INTRODUCTION.....	1
II. MATERIALS AND METHODS	
A. Animal Model.....	7
B. Experimental Protocol.....	7
C. Histology and Morphometric Analysis.....	8
D. Western Blot Analysis.....	9
III. RESULTS	
A. Hemodynamic Measurements.....	12
B. Morphometric Analysis.....	13
C. PPAR- $\gamma$ Protein Expression.....	14
IV. DISCUSSION.....	32
V. REFERENCE LIST.....	37
VI. VITA.....	44

## LIST OF ILLUSTRATIONS

Figure		Page
1.	Blood Vessel Morphometric Analysis Technique.....	11
2.	Treprostinil does not reduce RVSP in a rat model of MCT-induced pulmonary hypertension.....	17
3.	Treprostinil does not attenuate right ventricular hypertrophy in MCT-induced pulmonary hypertensive rats.....	19
4.	RVSP and RV/(LV+septum) measurements exhibit a direct correlation.....	21
5.	MCT induces medial wall thickness in pulmonary arteries.....	23
6.	High-dose treprostinil abrogates smooth muscle hypertrophy in resistance vessels (50-100 $\mu\text{m}$ ).....	25
7.	MCT increases percent medial wall thickness in pulmonary arteries.....	27
8.	MCT significantly increases percent medial wall thickness in pulmonary resistance vessels.....	29
9.	PPAR- $\gamma$ levels decrease with treprostinil treatment in a rat model of pulmonary hypertension.....	31

## LIST OF ABBREVIATIONS

Abbreviation	Definition
15d-PGJ <sub>2</sub> .....	15-deoxy- $\Delta^{12,14}$ -Prostaglandin J <sub>2</sub>
BCA.....	Bicinchoninic Acid
cAMP.....	Cyclic <u>Adenosine Monophosphate</u>
EC.....	Endothelial Cell
Ed.....	External Diameter
FDA.....	United States Food and Drug Administration
HRP.....	Horseradish Peroxidase
Id.....	Internal Diameter
IP.....	Prostacyclin Surface Prostanoid Receptor
La.....	Luminal Area
LV+septum.....	Left Ventricle + Septum
MCT.....	Monocrotaline
MWT.....	Medial Wall Thickness
NYHA.....	New York Heart Association
mPAP.....	Mean Pulmonary Arterial Pressure
PGI <sub>2</sub> .....	Prostaglandin I <sub>2</sub> (Prostacyclin)
PPAR- $\alpha$ , - $\beta/\delta$ , - $\gamma$ .....	Peroxisome Proliferator-Activated Receptor- $\alpha$ , - $\beta/\delta$ , - $\gamma$
PVR.....	Pulmonary Vascular Resistance
RV.....	Right Ventricle
RVSP.....	Right Ventricular Systolic Pressure
Va.....	Vessel Area
(V)SMC.....	(Vascular) Smooth Muscle Cell
VVG.....	Verhoeff-Van Gieson

# EFFECTS OF TREPROSTINIL SODIUM IN A MONOCROTALINE-INDUCED RAT MODEL OF PULMONARY HYPERTENSION

Shena L. Latcham

Dr. Jeffrey W. Skimming and Dr. Vincent G. DeMarco, Thesis Supervisors

## ABSTRACT

Treprostinil is a prostacyclin analog currently used in the treatment of pulmonary hypertension. Although clinical studies show treprostinil to be a successful therapy for pulmonary hypertension, little information exists concerning the effects of treprostinil treatment *in vivo*. The purpose of this study is to elucidate the effects of treprostinil on right ventricular systolic pressure (RVSP), right ventricular hypertrophy and vascular remodeling in a rat model of MCT-induced pulmonary hypertension. Male, Sprague-Dawley rats were randomized to one of four treatment groups; control, monocrotaline (MCT) only, MCT with treprostinil treatment (MCT/TRE), and treprostinil treatment only (TRE). At the beginning of the experiment, rats received a one-time subcutaneous dose of MCT (60 mg/kg) or saline. Rats were then administered either treprostinil or placebo for 28-days. After 28-days of treprostinil treatment, we recorded RVSP and right ventricular size. In addition, paraffin embedded left whole lung tissues were used for morphometric analysis and right whole lung tissues were snap frozen in liquid nitrogen for protein analysis. As expected, MCT exposure caused a significant increase in RVSP and right ventricular hypertrophy. Morphometric analyses also indicated that MCT-exposure led to medial wall thickening of the pulmonary vasculature. Neither low-dose (10 ng/kg/min) nor high-dose (150 ng/kg/min) treprostinil therapy attenuated elevations of RVSP and right ventricular hypertrophy in pulmonary hypertensive rats. In addition, there was no attenuation of medial wall thickening when MCT-exposed rats also received

treprostinil treatment. Finally, treprostinil significantly lowered PPAR- $\gamma$  protein expression in MCT-exposed rats. In conclusion, we demonstrated that increases in RVSP, right ventricular hypertrophy and vascular remodeling associated with MCT-induced pulmonary hypertension are not attenuated with treprostinil therapy.

Additionally, we found that treprostinil attenuated the induction of PPAR- $\gamma$  protein levels in whole lung homogenates of MCT-exposed rats. Although we have not yet established that PPAR- $\gamma$  is an important therapeutic target for pulmonary hypertension, we speculate that further investigation of its role could reveal a mechanism in which PGI<sub>2</sub> elicits its effects on the pulmonary vasculature.

## **Introduction**

Pulmonary hypertension is a rare disease described by an elevation of pulmonary arterial pressure. Although identification of pulmonary hypertension often goes unrecognized for several years, at the time of diagnosis, mean survival is approximately 2.8 years (46). Eventually, elevation of sheer stresses and hydrostatic forces lead to increased pulmonary vascular tone and pulmonary vascular remodeling, causing right ventricular heart failure and death (6).

In healthy individuals, pulmonary vascular tone is controlled by a balanced release of vasoactive mediators. Patients suffering from pulmonary hypertension though, commonly exhibit an abnormal synthesis of a number of endothelial-derived vasoactive mediators. These alterations include increases in vasoconstrictors such as thromboxane (8) and endothelin (16), as well as decreases in the endothelial-derived vasodilators nitric oxide (15) and prostacyclin (PGI<sub>2</sub>) (54). The lack of vasodilator influence disrupts balanced intrapulmonary production of vasoactive mediators leading to an overwhelming vasoconstrictor presence that results in exaggerated vasoconstriction (8; 58), cellular proliferation (17; 29) and smooth muscle hypertrophy (1) of the pulmonary vasculature.

In addition to alterations in vascular tone, pulmonary hypertensive patients also tend to develop vascular remodeling of the pulmonary vasculature. In 1958, Edwards and Heath (13) provided an in-depth description of the vascular pathology in pulmonary hypertensive patients. They divided histological changes of the pulmonary vasculature into six grades, which varied depending on disease severity. Likewise, disease severity was determined by the degree of hypertrophy and/or hyperplasia of fibroblasts, smooth muscle cells, and endothelium that make up the vascular wall. More recent studies

demonstrate that vascular remodeling also includes extension of smooth muscle into normally non-muscular vessels, termed neomuscularization (37). Taken together, these histological alterations, involving the intima, media, and adventitia (7), result in luminal obstruction which can lead to progressive increases in right ventricular afterload and ultimately right ventricular failure (24).

Even though pulmonary hypertension is an incapacitating and life-threatening disease, treatment options are available. Conventional therapies for pulmonary hypertension include vasodilators, anticoagulants, inotropic agents, diuretics, oxygen, and transplantation (20). Most commonly, treatments are administered to either inhibit mediators that induce vasoconstriction, vascular proliferation, and remodeling or increase vasodilating factors and growth factor inhibitors (52). Perhaps the most widely used treatment regimen to date involves chronic administration of intravenous PGI<sub>2</sub> to induce vasodilation and alter vascular remodeling of the pulmonary vasculature. PGI<sub>2</sub> is primarily generated in vascular endothelial cells and plays a major role in regulating vascular tone (41). Additionally, PGI<sub>2</sub> decreases platelet aggregation (39) and inhibits vascular smooth muscle cell (VSMC) proliferation (28), both of which are associated with vascular remodeling. Hence, PGI<sub>2</sub> therapy for pulmonary hypertensive patients appears to address many factors, such as increased vasoconstriction and vascular remodeling, associated with the disease.

While PGI<sub>2</sub> is a viable treatment for pulmonary hypertension, the nature of its delivery system through an intravenous catheter presents patients with many potential difficulties. First, because of a short half-life (2 to 3 minutes), interruptions in PGI<sub>2</sub> delivery caused by catheter displacement or delivery pump malfunction leads to life-

threatening rebound vasoconstriction. Second, indwelling catheter sites commonly get infections that can sometimes be treated with antibiotics and at other times cause life-threatening sepsis (4; 34). Thus, the impracticality of PGI<sub>2</sub> therapy led to the development of several PGI<sub>2</sub> analogs. PGI<sub>2</sub> analogs, such as inhaled iloprost and oral beraprost, show a nearly identical efficacy profile to PGI<sub>2</sub>, but are superior because they exhibit longer bioavailabilities, require less complex delivery methods, and provide selectivity for the pulmonary circulation (22; 42; 48).

In 2002, the FDA approved another PGI<sub>2</sub> analog, treprostinil, as a treatment for patients suffering from New York Heart Association (NYHA) class II-IV pulmonary hypertension. Treprostinil functions as a long-acting, stable tricyclic benzindine analog of PGI<sub>2</sub>. Its desirable characteristics include chemical stability at room temperature, a neutral pH, and a half-life of 3-4 hours. More importantly, though, treprostinil is administered subcutaneously (57) rather than intravenously. This represents the most significant advantage of treprostinil over other PGI<sub>2</sub> analogs since the risk of catheter site infection and rebound vasoconstriction due to catheter displacement are eliminated. Treprostinil-treated patients also experience similar improvements in mean right atrial pressure, mean pulmonary arterial pressure (mPAP), cardiac index, and pulmonary vascular resistance (PVR) when compared to patients using alternate PGI<sub>2</sub> analogs for pulmonary hypertension. Additionally, treprostinil consistently improves exercise capacity, indices of dyspnea, signs and symptoms of pulmonary arterial hypertension, cardiopulmonary hemodynamics, and the physical dimension of quality of life (50). Although clinical trials show that treprostinil is a successful treatment, little is known

about how treprostinil, and PGI<sub>2</sub> in general, work at a cellular level to alleviate symptoms associated with pulmonary hypertension.

Recently, Narumiya, et. al. (38), revealed that PGI<sub>2</sub> could function by binding cell surface prostanoid receptors (IP) that activate adenylate cyclase through the G-protein, G<sub>s</sub>. Once activated, adenylate cyclase stimulates the release of cyclic-AMP (cAMP) to reduce intracellular calcium levels, which results in relaxation of the vascular smooth muscle in the pulmonary vasculature. Although PGI<sub>2</sub> may cause cAMP-induced relaxation via the IP receptor, no IP receptor antagonists are currently available, therefore it cannot be determined if PGI<sub>2</sub> functions exclusively through IP receptors (9; 40).

Hatae, et al. (18), subsequently found that PGI<sub>2</sub> also works via peroxisome proliferator-activated receptor (PPAR)- $\delta$ . Likewise, they showed that once PGI<sub>2</sub> binds to PPAR- $\delta$ , PGI<sub>2</sub> induces apoptosis in a PPAR- $\delta$  dependent manner and independently of the IP receptor-signaling pathway. Thus, studying the effects of PGI<sub>2</sub> ligand binding to PPARs could provide more insight into the means in which PGI<sub>2</sub> and its analogs induce vasodilation and alter vascular remodeling of the pulmonary vasculature.

PPARs belong to the super family of nuclear receptors made up of three subtypes: PPAR- $\alpha$ , - $\beta/\delta$ , and - $\gamma$ . PPARs as a whole operate as ligand-activated transcription factors (30) that once bound to promoter regions of specific target genes, can alter gene expression (44). Although PPARs are traditionally associated with adipocyte differentiation, recently PPAR- $\gamma$  also was found in VSMCs (32), ECs (31), and macrophages (53) of the vascular wall, indicating that PPAR- $\gamma$  might participate in cardiovascular disease. Accordingly, Bishop-Bailey, et al., (5), demonstrated that ligand-bound PPAR- $\gamma$  beneficially effects the vasculature by inhibiting inflammatory cell

responses, reducing proliferation and migration of VSMCs *in vitro*, and diminishing atherosclerotic lesion development and neointimal formation *in vivo*. These data suggest that PPAR- $\gamma$  could play a role in pulmonary hypertension by decreasing vascular remodeling in the lungs, thereby reducing vascular resistance and increasing blood vessel volume (25).

Although it remains unknown whether or not PGI<sub>2</sub> and its analogs act as PPAR- $\gamma$  ligands, many similarities between the actions of PGI<sub>2</sub> and PPAR- $\gamma$  in the vasculature warrants further investigation. For instance, 15-deoxy- $\Delta^{12,14}$ -Prostaglandin J<sub>2</sub> (15d-PGJ<sub>2</sub>), the natural ligand to PPAR- $\gamma$ , and PGI<sub>2</sub> are both cyclooxygenase products produced by the breakdown of prostaglandin H<sub>2</sub>. PGI<sub>2</sub> production also occurs in the vascular endothelium, which makes it readily available to activate PPAR- $\gamma$  receptors found in VSMCs, ECs, and macrophages of the vasculature. Finally, activated PPAR- $\gamma$  and PGI<sub>2</sub> perform similarly in the vasculature by reducing the inflammatory response, inhibiting vascular remodeling, and inducing cell apoptosis. Therefore, investigating the influence of PGI<sub>2</sub> on PPAR- $\gamma$  could reveal a mechanism by which PGI<sub>2</sub> induces beneficial effects on the pulmonary vasculature in pulmonary hypertensive patients.

In the present study, our lab elected to use an established rat model of monocrotaline (MCT)-induced pulmonary hypertension. The primary rationale for using this model stems from certain similarities between MCT-induced pulmonary hypertension in animals to that seen with pulmonary hypertensive disease progression in humans. For example, MCT, a pyrrolizidine alkaloid, causes endothelial cell injury, which leads to a mononuclear infiltration into the perivascular regions of the arterioles and muscular arteries (12; 47). MCT also increases mPAP, induces right ventricular hypertrophy,

increases the medial and adventitial thickness of muscular arteries, and enhances the appearance of muscle in normally non-muscular arteries (26). Additionally, several studies confirm that PGI<sub>2</sub> treatment successfully attenuates elevations in mPAP (3), right ventricular systolic pressure (RVSP) (56), and right ventricular hypertrophy (55; 56) associated with MCT-induced pulmonary hypertension.

Therefore, using a rat model of MCT-induced pulmonary hypertension, our lab sought to elucidate the effects of treprostinil on the hemodynamics and vascular remodeling of the pulmonary vasculature. We also evaluated PPAR- $\gamma$  protein expression with and without treprostinil treatment in order to gain a better understanding of the role that PPAR- $\gamma$  plays in pulmonary hypertension. We hypothesized that (1) treprostinil induces vasodilation of the pulmonary vasculature causing a decrease in RVSP (2) treprostinil attenuates overpressurization and overcirculation in the lungs leading to lessened right ventricular hypertrophy, and (3) treprostinil diminishes vascular remodeling by attenuating increases of medial wall thickness, potentially via a PPAR- $\gamma$ -dependent mechanism.

## Materials and Methods

### **I. Animal Model**

Male, Sprague-Dawley rats (325-375 grams) were purchased from Harlan Laboratories (Indianapolis, IN). Rats were fed a standard laboratory chow and given water *ad libitum* for the duration of the experiment. The Institutional Animal Use and Care Committee of the University of Missouri-Columbia approved of the experiments, and the care and handling of the animals were in accordance with the National Institutes of Health guidelines. Prior to surgery, rats were randomized into four treatment groups: Control, MCT only, MCT plus treprostinil treatment, and treprostinil treatment only. Rats were anesthetized with a ketamine (80 mg/kg) and xylazine (8 mg/kg) cocktail by way of a hind limb intramuscular injection. Once anesthetized, a 200  $\mu$ L osmotic pump (DURECT Corp., Cupertino, CA) was inserted subcutaneously into the nape of the neck to deliver either treprostinil (10 ng/kg/min or 150 ng/kg/min) or placebo at a rate of 0.25  $\mu$ L/hour for 28 days. A one-time subcutaneous dose of either 0.9% saline or MCT (60 mg/kg) was also given at the time of pump implantation.

### **II. Experimental Protocol**

Twenty-eight days post-pump implantation, rats were anesthetized with a ketamine/xylazine cocktail. A tracheotomy was performed, and a 14-gauge catheter was secured in the trachea and attached to a Harvard model 683 small animal ventilator (Harvard Apparatus, South Natick, MA). The ventilator was adjusted to deliver 4 mL of room air 35 times per minute. A Millar catheter (Millar Instruments, Model SPR-534, Houston, TX) was then inserted into the right jugular vein and advanced into the right ventricle for continuous right ventricular systolic (RVSP) monitoring, an indicator of

mPAP, using a polygraph (BIOPAC Systems, Model MP 100, Santa Barbara, CA). Next, rats were euthanized by removing the heart and lungs *en bloc*. The heart was dissected into the right ventricle and the left ventricle plus septum according to methods described by Cottrill, et al. (10). Right ventricular (RV) free wall and left ventricular free wall plus the septum (LV+septum) were weighed. Weights were applied to the equation  $[RV/(LV+septum)]$  to obtain an estimate of right ventricular hypertrophy. Next, the lungs were inflated with 10 mL of ambient air in situ and then the airway was tied off. While still inflated, the right lung was immediately immersed in 10% neutral buffered formalin. The left lung was snap frozen in liquid nitrogen and stored at  $-80^{\circ}\text{C}$  for subsequent protein analysis. Finally, osmotic pumps were removed to assess the amount of either placebo or treprostinil remaining inside the pump. All pumps contained less than 10  $\mu\text{L}$  of fluid indicating that all pumps functioned properly throughout the duration of the experiment.

### **III. Histology and Morphometric Analysis**

Right lung tissue was formalin fixed for 24 hours, paraffin embedded, cut into 4  $\mu\text{m}$  sections and mounted on glass slides. Sections were stained for elastic fibers using Verhoeff-Van Gieson (VVG) stain. In order to determine the amount of thickening that occurred in the tunica media of vessels as a consequence of pulmonary hypertension, morphometric analyses were conducted on all tissue slides using a method described by Geraci, et al. (14). Briefly, measurements of the external and luminal diameter were taken and expressed as a ratio of vessel diameter by the equation  $(E_d - I_d)/E_d$ , where  $E_d$  denotes the external diameter and  $I_d$  denotes the internal diameter. External diameters were calculated by making a linear measurement from the external elastic lamina on one

side of the vessel to the external elastic lamina on the other side of the vessel. Similarly, luminal diameter was calculated using linear measurements made from the internal elastic lamina on one side of the lumen to the internal elastic lamina on the other side of the lumen (Figure 1a). For both the Ed and Id, three measurements were taken, averaged, and recorded. The recorded vessel Ed and Id were then applied to the equation  $(Ed - Id)/Ed$  in order to obtain a measurement of medial wall thickness (MWT). Additionally, only transversely cut vessels that were either concentric or nearly concentric were used. Approximately 10-25 vessels were measured per animal.

A second morphological technique also was utilized to verify results obtained by the linear measurement method previously described. Using Image Pro® Plus software (Media Cybernetics Inc, Silver Spring, MD), vessel smooth muscle area was calculated by the equation  $[(Va - La)/Va * 100]$ , where Va denotes the entire vessel area and La denotes the luminal area (Figure 1b). Smooth muscle area was expressed as a percentage of the whole vessel size. No vessels were excluded in smooth muscle area measurements. Thirty-five vessels were measured per animal.

#### **IV. Western Blot Analysis**

Lung tissue was thawed and homogenized in lysis buffer (50 mM Tris-HCl, 0.1 mM EDTA, 0.1 mM EGTA, 0.1%  $\beta$ -mercaptoethanol, 1 mM PMSF, 2  $\mu$ mol leupeptin, 1  $\mu$ mol pepstatin A, 20 mM CHAPS, and 10% glycerol) at 4°C. Crude homogenates were centrifuged at 16,000g for 6 minutes at 15°C to remove remaining tissue fragments. Supernatants were retained for protein analysis. The supernatant protein concentration was determined using a BCA Protein Assay Kit (Pierce Chemical Co., Rockford, IL). For each sample, 10  $\mu$ g of protein were added to an equal volume of 2X sample buffer

(250 mM Tris pH=6.8, 4% SDS, 10% glycerol, 0.006% bromophenol blue, 2%  $\beta$ -mercaptoethanol), boiled 5 minutes, and loaded onto a 4-20% Tris-HCl Minigel (Biorad). Proteins were separated by gel electrophoresis performed at 100V for 60 minutes. Proteins were then electrotransferred onto a nitrocellulose membrane at 100V for 30 minutes. The nitrocellulose membranes were immediately placed into blocking buffer (5.0% non-fat dry milk, 10 mM Tris pH=7.5, 100 mM sodium chloride, 0.1% Tween-20) and incubated at room temperature one hour. After blocking, membranes were incubated in rabbit polyclonal anti-PPAR- $\gamma_1$  and - $\gamma_2$  (Biomol Research Laboratories, Plymouth Meeting, PA), diluted 1:3000 in blocking buffer, overnight at 4<sup>0</sup>C. Membranes were then incubated with anti-rabbit Ig, HRP (Amersham Biosciences, Piscataway, NJ), diluted 1:2000 in blocking buffer, for one hour at room temperature. PPAR- $\gamma$  protein bands were visualized by chemiluminescence (ECL detection kit, Amersham Biosciences, Piscataway, NJ) at 60 kDa. Densitometric analysis of PPAR- $\gamma$  was conducted using Adobe Photoshop v7.0 software (Adobe Systems Incorporated, San Jose, CA).

### **Statistical Analysis**

Statistical analyses were performed using SigmaStat for Windows, Version 2.03 (SPSS, Chicago, IL). Differences among the means of the groups were identified using a one-way analysis of variance. Post-hoc analyses using Fischer's LSD were conducted if the analysis of variance detected an effect of treatment. A significance level was set as  $p \leq 0.05$ . Data are reported as means  $\pm$  SD.

## Blood Vessel Morphometric Analysis Technique Comparison

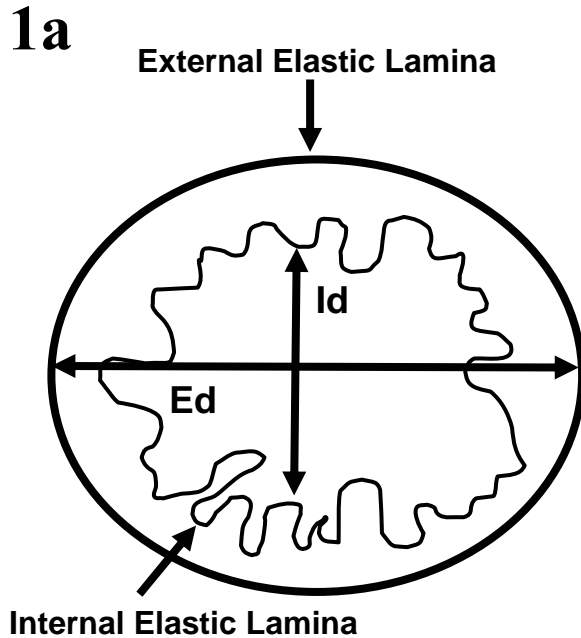


**Figure 1a. Morphometric analysis using linear measurements.** External diameter (Ed) was calculated by making a linear measurement from the external elastic lamina on one side of the vessels to the external elastic lamina on the other side of the vessel. Internal diameter (Id) was calculated similarly using the internal elastic lamina. For both Ed and Id, three measurements were taken and then averaged for each vessel. Average Ed and Id were then applied to the equation  $(Ed-Id)/Ed$  to obtain a measurement of MWT.

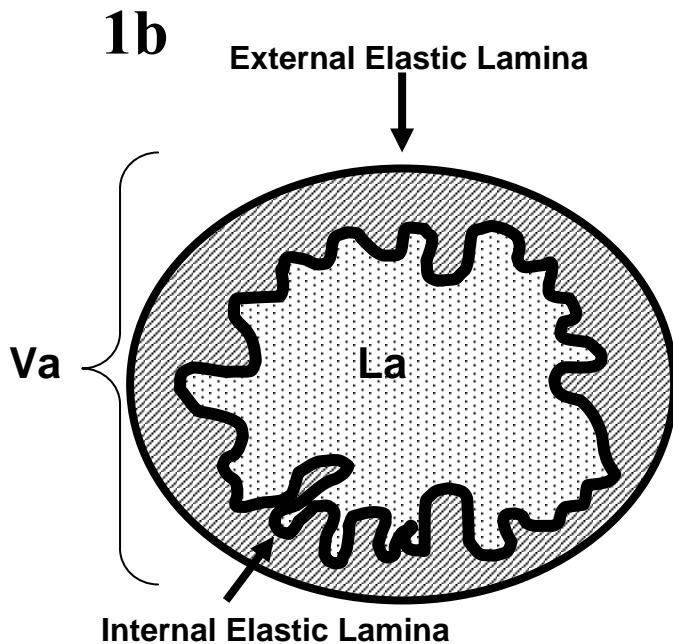


**Figure 1b. Morphometric analysis using area measurements.** Image Pro® Plus software was used to calculate whole vessel area (Va), and vessel luminal area (La). The Va (lines + dots) includes the external elastic lamina and all area inside it. The La (dots) includes the internal elastic lamina and the area it encloses. Percent vessel smooth muscle area (lines) was calculated by the equation  $[(Va-La)/Va * 100]$ .

## Results

### I. Hemodynamic Measurements

RVSP was significantly higher in all rats that received MCT only when compared to control rats ( $35.6 \pm 5.44$  versus  $25.2 \pm 4.21$  mm Hg,  $p < 0.01$ , in Figure 2a, and  $42.3 \pm 10.5$  versus  $29.1 \pm 2.14$  mm Hg,  $p < 0.01$ , in Figure 2b). Additionally, MCT only rats showed significantly higher RVSPs when compared to rats that received either low-dose ( $35.6 \pm 5.44$  versus  $25.0 \pm 1.30$  mmHg,  $p < 0.004$ ) or high-dose ( $42.3 \pm 10.5$  versus  $25.7 \pm 1.63$  mm Hg,  $p < 0.001$ ) treprostinil alone. In contrast, there were no significant differences in RVSP between rats that received MCT alone and rats administered MCT and either low-dose (Fig. 2a) or high-dose treprostinil (Fig. 2b). There were also no changes in RVSP between control and treprostinil only groups regardless of the treprostinil dose. These data indicate that MCT, but not treprostinil, induces an elevation of RVSP. Likewise, treprostinil treatment does not reduce elevated RVSP in MCT-treated rats.

At necropsy, we obtained measurements of right ventricular hypertrophy by comparing the weight of the RV to the weight of the LV+septum. Rats that received MCT had a significantly higher RV/(LV+septum) ratio when compared to controls ( $0.33 \pm 0.05$  versus  $0.25 \pm 0.02$ ,  $p < 0.003$ , in figure 3a, and  $0.33 \pm 0.05$  versus  $0.26 \pm 0.02$ ,  $p < 0.003$ , in figure 3b) indicating that MCT induces right ventricular hypertrophy. Conversely, neither low-dose (Figure 3a) nor high-dose treprostinil treatment (Figure 3b) lessened the right ventricular size seen in rats that also received MCT. Moreover, there were no significant differences in right ventricular size between control and either low- or high-dose treprostinil only rats. We therefore concluded that MCT alone induces right ventricular hypertrophy and that treprostinil is unable to abrogate the effects of MCT.

Furthermore, treprostinil alone does not affect right ventricular size. Linear regression analysis though, revealed a positive correlation between increasing right ventricular hypertrophy and RVSP (Figure 4).

### **III. Morphometric Analysis**

Using a linear measurement morphometric model, we found that all rats which received MCT showed significant increases in MWT when compared to controls ( $0.394 \pm 0.07$  versus  $0.268 \pm 0.06$ ,  $p < 0.01$ ) and treprostinil only rats ( $0.394 \pm 0.07$  vs.  $0.207 \pm 0.01$ ,  $p < 0.001$ ) (Figure 5). However, treprostinil treatment did not decrease MWT in the pulmonary arteries of rats with MCT-induced pulmonary hypertension. Additionally, although a trend was observed, MWT did not significantly vary between control and treprostinil only rats. Next, we grouped vessels by size based on external diameter; a)  $< 50 \mu\text{M}$ , b)  $50\text{-}100 \mu\text{M}$ , c)  $100.1\text{-}200 \mu\text{M}$ , and d)  $> 200 \mu\text{M}$  and again calculated MWT by the equation  $(\text{Ed}-\text{Id})/\text{Ed}$  (Figure 6). MCT significantly increased MWT in vessels of size  $< 50 \mu\text{M}$  ( $0.405 \pm 0.10$  versus  $0.268 \pm 0.11$ ,  $p < 0.001$ ) and  $50\text{-}100 \mu\text{M}$  ( $0.427 \pm 0.11$  versus  $0.228 \pm 0.10$ ,  $p < 0.001$ ) when compared to vessels of the same size from control rats. In addition, high-dose treprostinil significantly attenuated MCT-induced increases in MWT of resistance vessels  $50\text{-}100 \mu\text{M}$  in size ( $0.377 \pm 0.11$  versus  $0.427 \pm 0.11$ ,  $p < 0.002$ ). Treprostinil treatment alone also lessened MWT in vessels that were  $< 50 \mu\text{M}$ ,  $50\text{-}100 \mu\text{M}$ , and  $100.1\text{-}200 \mu\text{M}$  when compared to controls, although a significant reduction was seen only in pulmonary vessels  $100.1\text{-}200 \mu\text{M}$  in diameter ( $0.224 \pm 0.09$  versus  $0.331 \pm 0.14$ ,  $p < 0.001$ ). Pulmonary vessels  $> 200 \mu\text{M}$  showed no significant differences in MWT between any of the treatment groups. Hence, treprostinil appears to reduce MWT to a

greater degree in resistance vessels rather than in conduit vessels of the pulmonary vasculature.

Next, we measured MWT using a second morphometric technique that calculates the percent smooth muscle area of each vessel in relation to the entire vessel area,  $[(Ea-Ia)/Ea * 100]$ . This ratio gives us the % MWT of each artery (Figure 7). All transversely cut vessels, regardless of shape or size, were included in the analysis. MCT significantly increased % MWT in vessels of all sizes when compared to controls ( $44.9\% \pm 6.01$  versus  $33.8\% \pm 5.81$ ,  $p < 0.008$ ), but treprostinil treatment did not abrogate the effects of MCT. Next, we grouped pulmonary vessels according to size; a)  $< 50 \mu\text{M}$ , b)  $50-100 \mu\text{M}$ , c)  $100.1-200 \mu\text{M}$ , and d)  $> 200 \mu\text{M}$  and analyzed % MWT of each vessel (Figure 8). Treprostinil only treatment significantly decreased % MWT in resistance vessels  $50-100 \mu\text{m}$  in size when compared to control vessels ( $27.5\% \pm 3.28$  versus  $33.3\% \pm 6.00$ ,  $p < 0.001$ ). Contradictory to our linear measurement analysis though, we could not find a significant attenuation of % MWT in vessels of any size, including  $50-100 \mu\text{m}$ , when MCT-induced pulmonary hypertensive rats were treated with high-dose treprostinil. Because these outcomes opposed those found by our initial morphometric analysis, we reevaluated the data and determined that an alpha-error was made in our linear measurement results. Likewise, we resolved that the area measurements represent the vessel MWT most accurately. Hence, using area measurements, we established that treprostinil does not attenuate MCT-induced increases in % MWT.

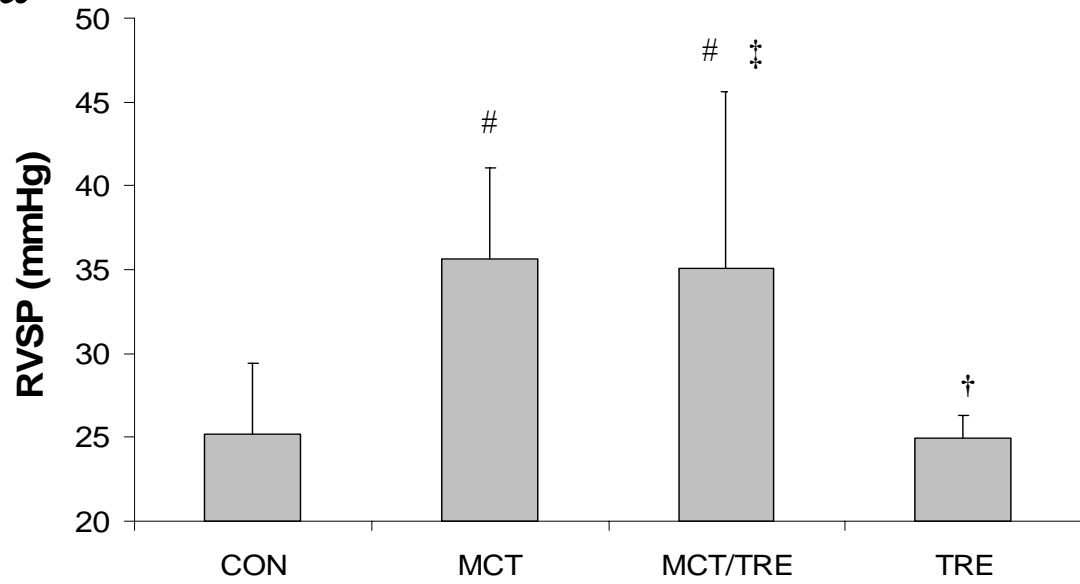
#### **IV. PPAR- $\gamma$ Protein Expression**

Finally, we examined the effects of treprostinil on PPAR- $\gamma$  protein levels in whole lung homogenates (Figure 9). Densitometric analysis of Western blots revealed that

MCT increased PPAR- $\gamma$  levels in the lung in comparison to controls ( $37.5 \pm 6.95$  versus  $20.4 \pm 1.52$ ,  $p=0.001$ ). Treprostinil treatment also significantly reduced PPAR- $\gamma$  protein expression when compared to rats administered MCT alone ( $27.36 \pm 7.78$  versus  $37.47 \pm 6.95$ ,  $p=0.03$ ). Additionally, there were no measurable differences between control, treprostinil-treated pulmonary hypertensive rats, and treprostinil only rats.

**Figure 2. Treprostinil does not reduce RVSP in a rat model of MCT-induced pulmonary hypertension.** (2a) Low-dose treprostinil (10 ng/kg/min), (2b) High-dose treprostinil (150 ng/kg/min). Mean  $\pm$  SD RVSP in control (CON), MCT only, MCT with treprostinil treatment (MCT/TRE), and treprostinil only (TRE) rats were measured 28-days post-osmotic pump implantation. MCT only rats exhibited significantly elevated RVSPs. Treprostinil did not reduce the RVSP of rats that received both MCT and either low-dose or high-dose treprostinil when compared to rats that received MCT alone. #  $p < 0.01$  vs. CON, \*  $p < 0.001$  vs. MCT, †  $p = 0.004$  vs MCT, ‡  $p < 0.009$  vs. TRE.

**2a**



**2b**

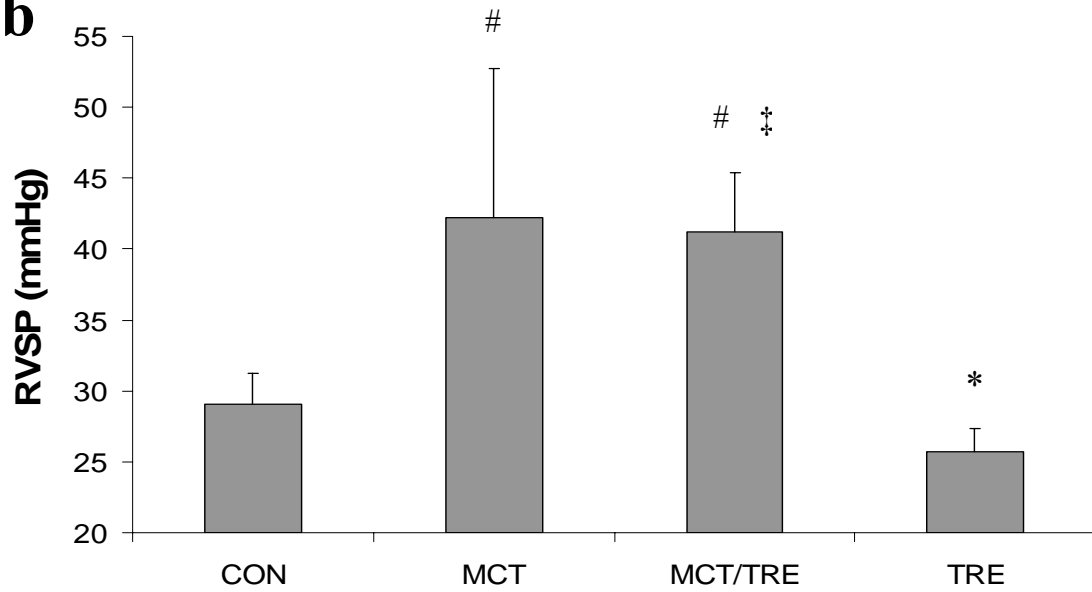
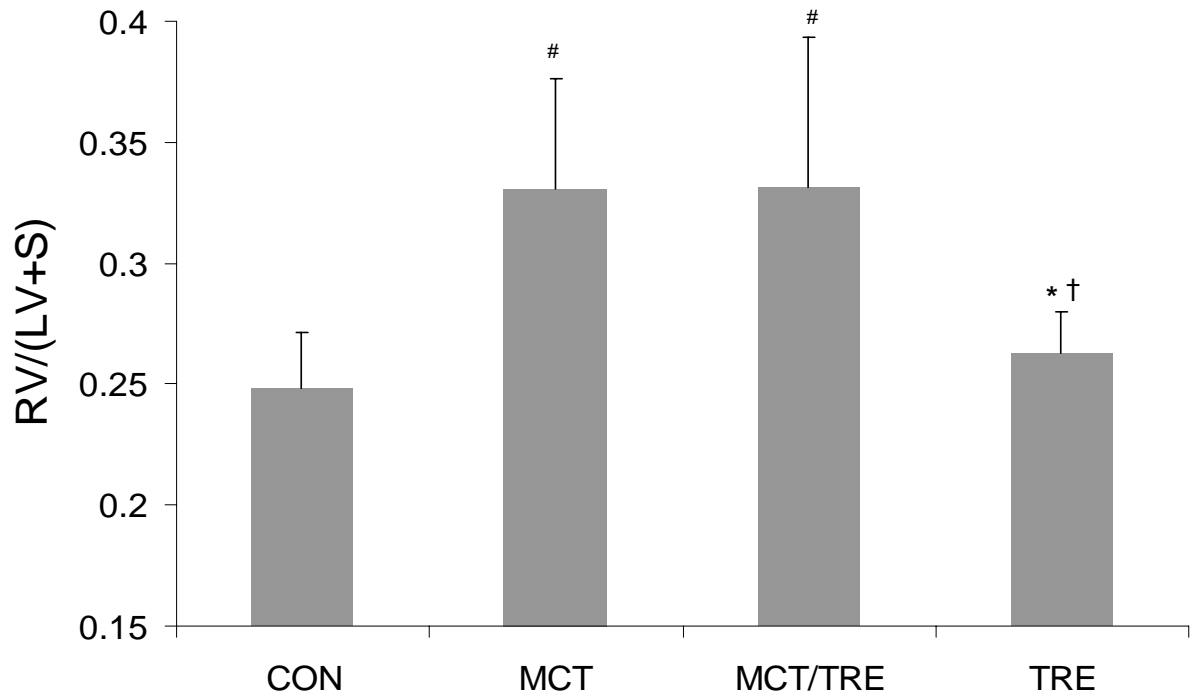


**Figure 3. Treprostinil does not attenuate right ventricular hypertrophy in MCT-induced pulmonary hypertensive rats.** (3a) Low-dose treprostinil (10 ng/kg/min), (3b) High-dose treprostinil (150 ng/kg/min). Mean  $\pm$  SD right ventricular size was measured on rat hearts dissected into the RV and the LV+septum in control (CON), MCT only, MCT with treprostinil treatment (MCT/TRE), and treprostinil only (TRE) rats. All rats treated with MCT exhibited a significantly higher right ventricular size when compared to control or treprostinil only rats. Treprostinil treatment was unable to attenuate MCT-induced right ventricular hypertrophy. #  $p < 0.003$  vs CON, \*  $p < 0.008$  vs MCT, †  $p = 0.008$  vs. MCT/TRE, ‡  $p < 0.001$  vs. MCT/TRE.

**3a**



**3b**

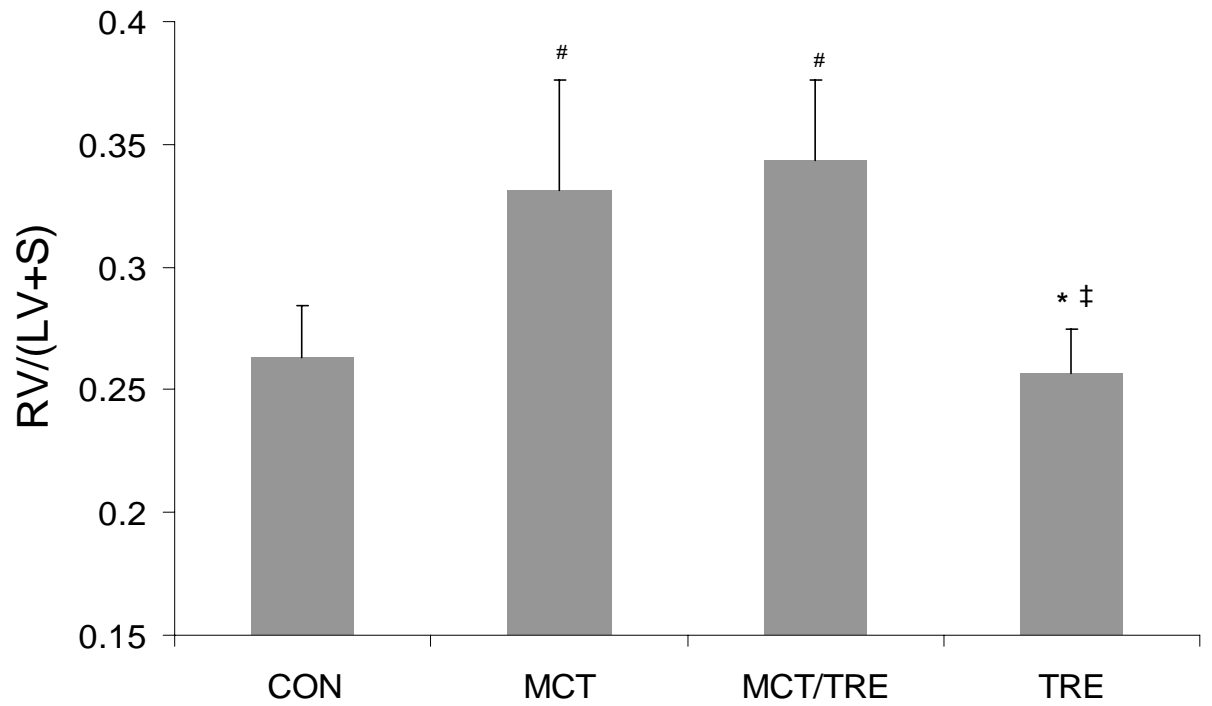


**Figure 4. RVSP and RV/(LV+septum) measurements exhibit a positive correlation.** Correlation between RVSP and right ventricular hypertrophy measured by heart dissection is shown in control, MCT only, MCT with treprostinil treatment (MCT/TRE), and treprostinil only (TRE) rats. The following regression equation was obtained:  $RVSP \text{ (mm Hg)} = 141.08 * X - 9.4188$ .  $R^2 = 0.7134$ ,  $n = 56$ .

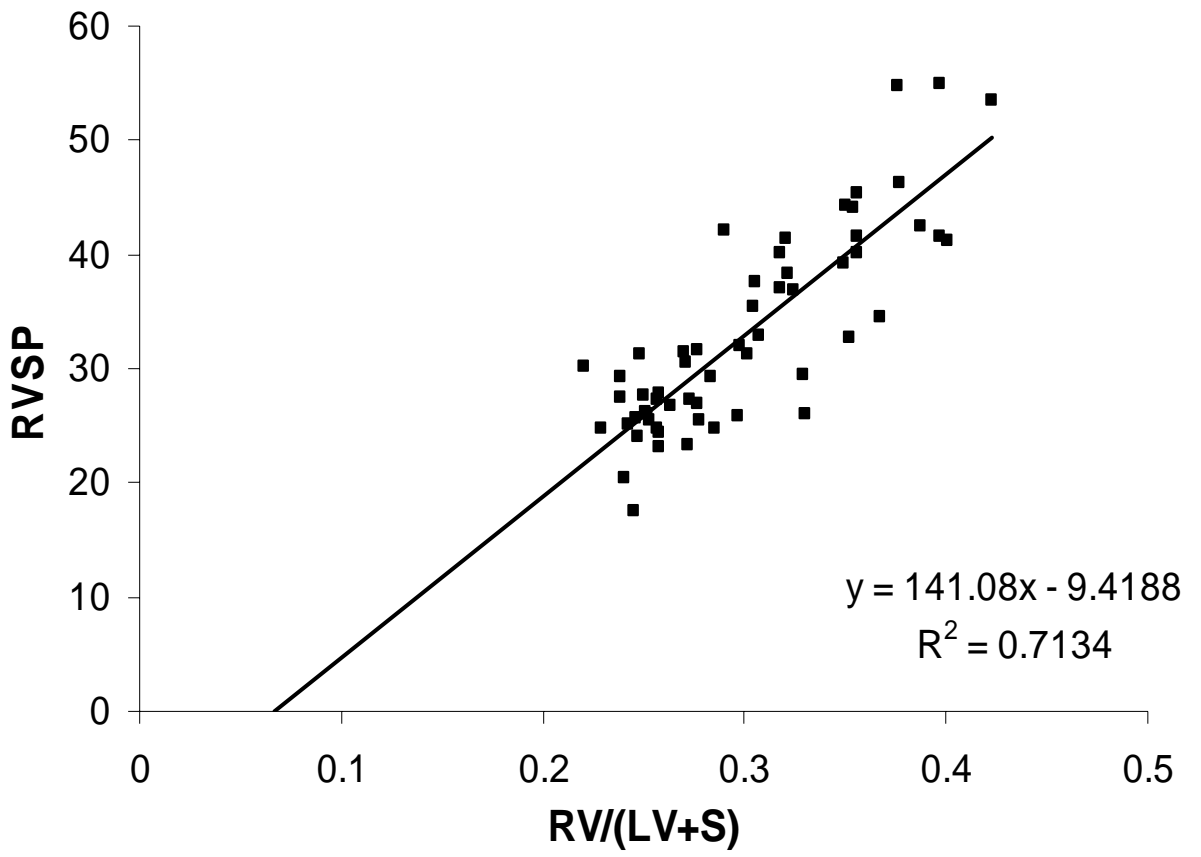


**Figure 5. MCT induces medial wall thickness in pulmonary arteries.** Lung sections were subjected to VVG staining and analyzed via the linear measurement equation,  $(Ed-Id/Ed)$ . Vessels of varied sizes were divided into four groups depending on treatment received; control (CON), MCT only, MCT with treprostinil treatment (150 ng/kg/min) (MCT/TRE), and treprostinil only (TRE). Approximately 10-25 vessels were measured per animal. Medial wall thickness (MWT) of pulmonary arteries was significantly increased in all rats receiving MCT. Treprostinil did not significantly attenuate the effects of MCT on increased MWT. †  $p < 0.001$  vs TRE, #  $p < 0.008$  vs CON.

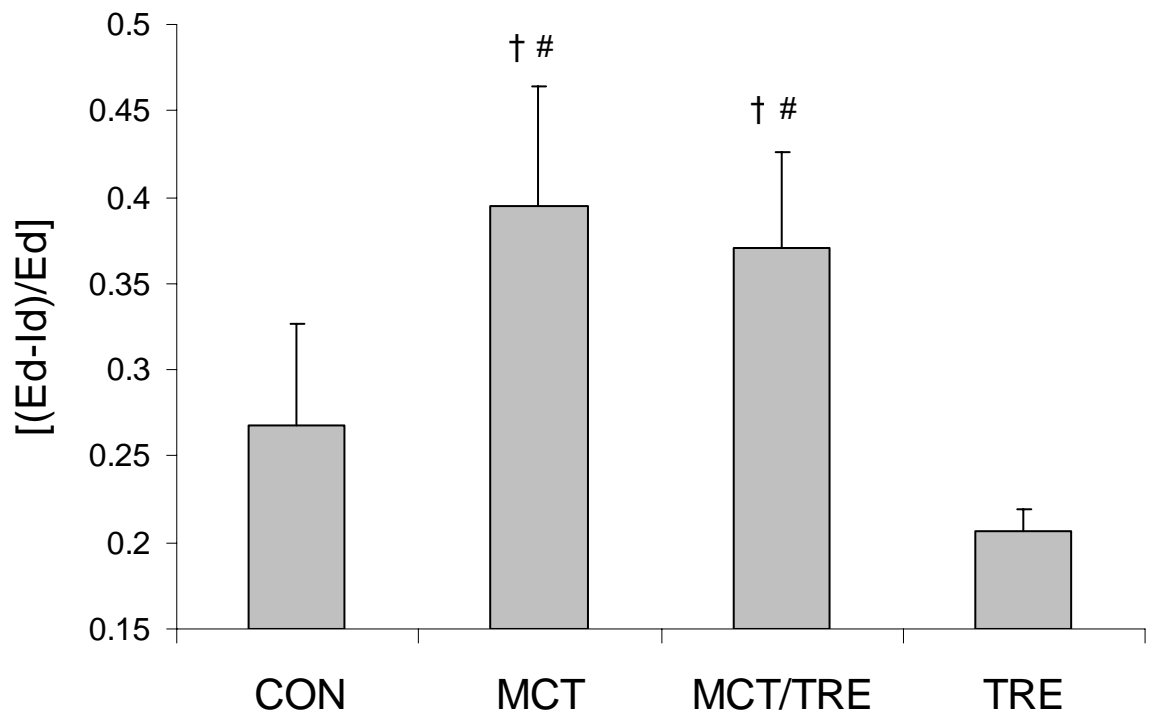


**Figure 6. High-dose treprostinil abrogates smooth muscle hypertrophy in resistance vessels (50-100  $\mu\text{m}$ ).** Pulmonary arteries were measured and analyzed via the linear relationship  $(\text{Ed}-\text{Id})/\text{Ed}$ . Vessels were then assigned to one of four groups according to size;  $<50 \mu\text{m}$ ,  $50-100 \mu\text{m}$ ,  $100-200 \mu\text{m}$ , and  $>200 \mu\text{m}$ . Rats receiving MCT showed significantly more medial wall thickening (MWT) in vessels  $<50 \mu\text{m}$  and  $50-100 \mu\text{m}$  in size. Treprostinil significantly decreased MCT-induced MWT in pulmonary arteries ranging from  $50-100 \mu\text{m}$  ( $p=0.01$ ). There were no changes between treatment groups for vessels  $>200 \mu\text{m}$ . \*  $p < 0.005$  vs. M/T, \*\*  $p = 0.01$  vs MCT, #  $p < 0.001$  vs. CON, †  $p < 0.002$  vs. MCT, ‡  $p < 0.001$  vs. TRE.

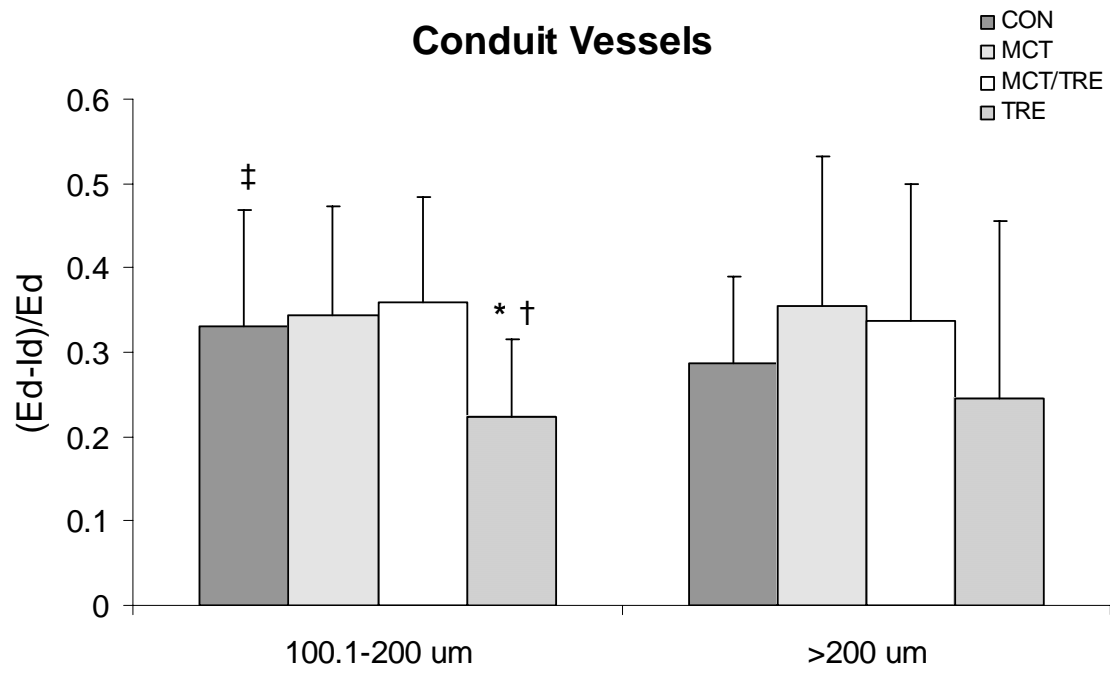
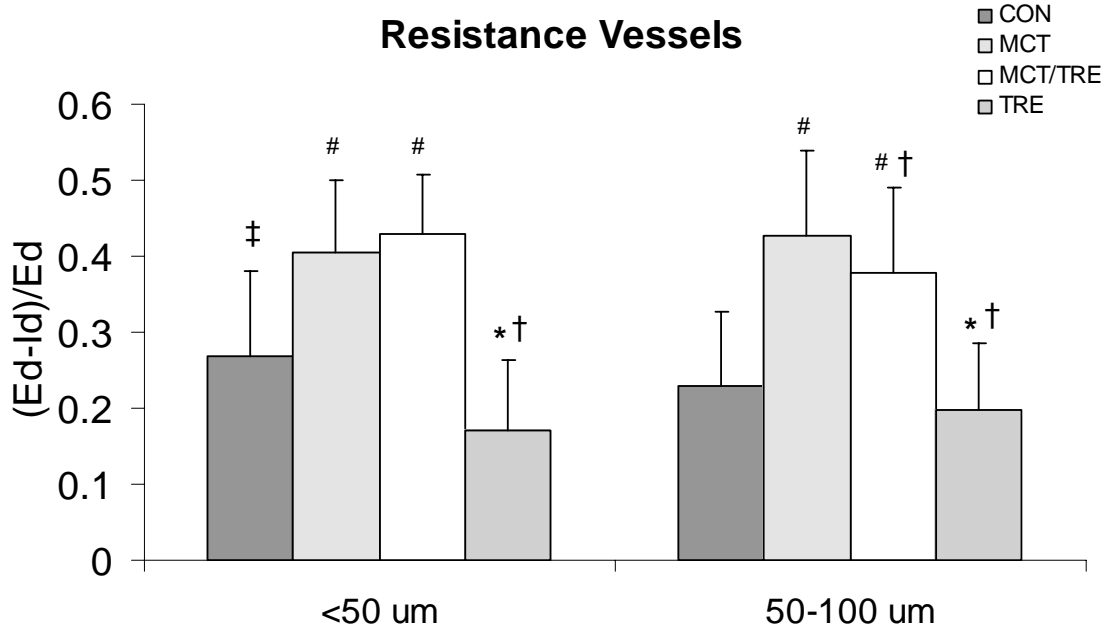


**Figure 7. MCT increases percent medial wall thickness in pulmonary arteries.**

Whole rat lung sections were stained with VVG then analyzed via the area relationship  $[(Ea-Ia)/Ea*100]$ . Vessels of selected size ranges were divided into four groups depending on treatment received; control (CON), MCT only, MCT with treprostinil treatment (MCT/TRE), and treprostinil only (TRE). Thirty-five vessels were measured per animal. Percent medial wall thickness (% MWT) of pulmonary arteries was significantly increased in all rats receiving MCT. Treprostinil did not attenuate the effects of MCT on % MWT. †  $p<0.001$  vs TRE, #  $p<0.008$  vs CON.

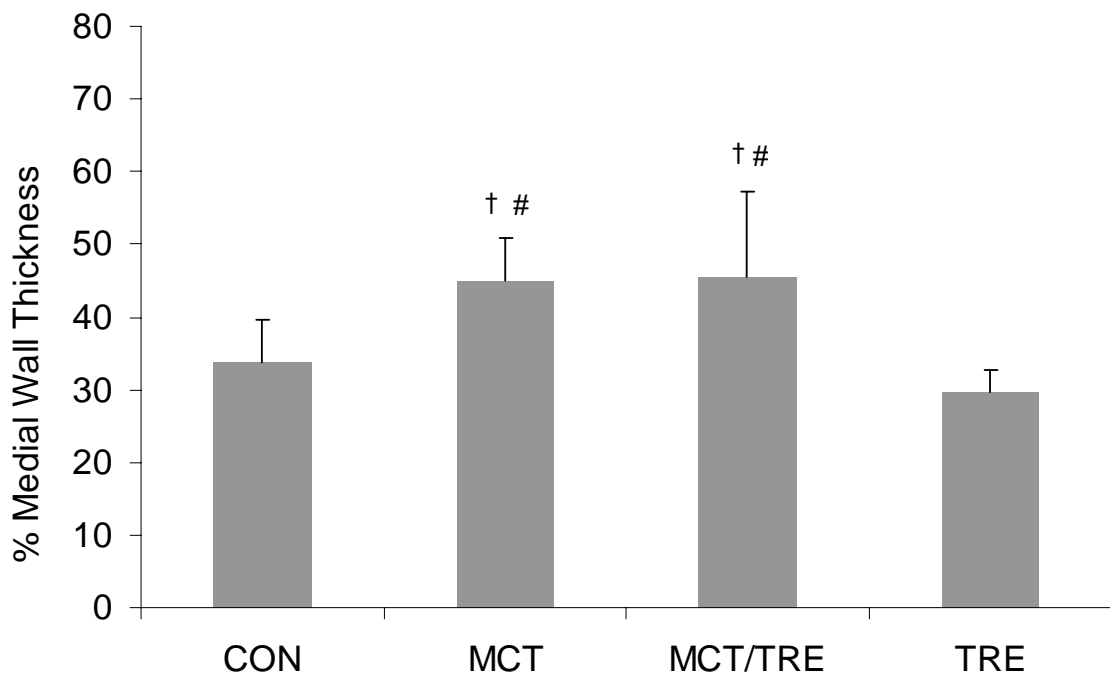


**Figure 8. MCT significantly increases percent medial wall thickness in pulmonary resistance vessels.** Vessels from whole rat lung were assigned to one of four groups according to size; <50  $\mu\text{m}$ , 50-100  $\mu\text{m}$ , 100-200  $\mu\text{m}$ , and >200  $\mu\text{m}$ . Rats receiving MCT exhibited a significant increase in percent medial wall thickness (% MWT) in resistance vessels <50  $\mu\text{m}$  or >200  $\mu\text{m}$  in size. Treprostinil did not reduce MCT-induced increases in % MWT in pulmonary arteries ranging from 50-100  $\mu\text{m}$  ( $p=0.01$ ). There was no variation in % MWT between groups in vessels >200  $\mu\text{m}$  (data not shown).

\*  $p < 0.005$  vs. M/T, #  $p < 0.001$  vs. CON, †  $p < 0.002$  vs. MCT, ‡  $p < 0.001$  vs. TRE.

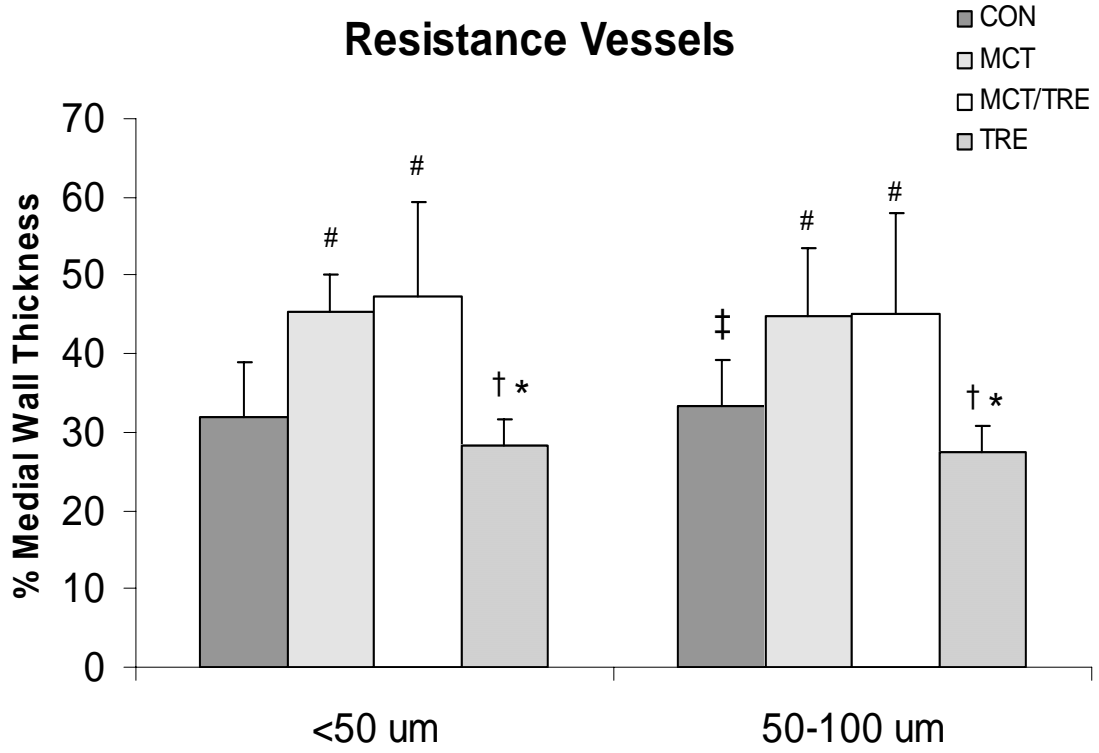
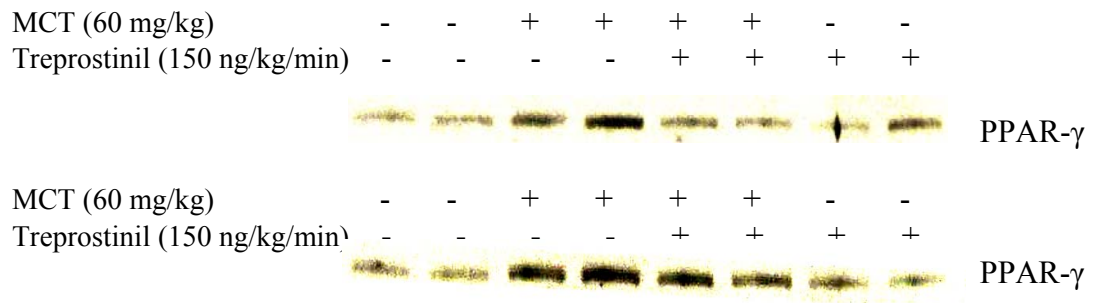
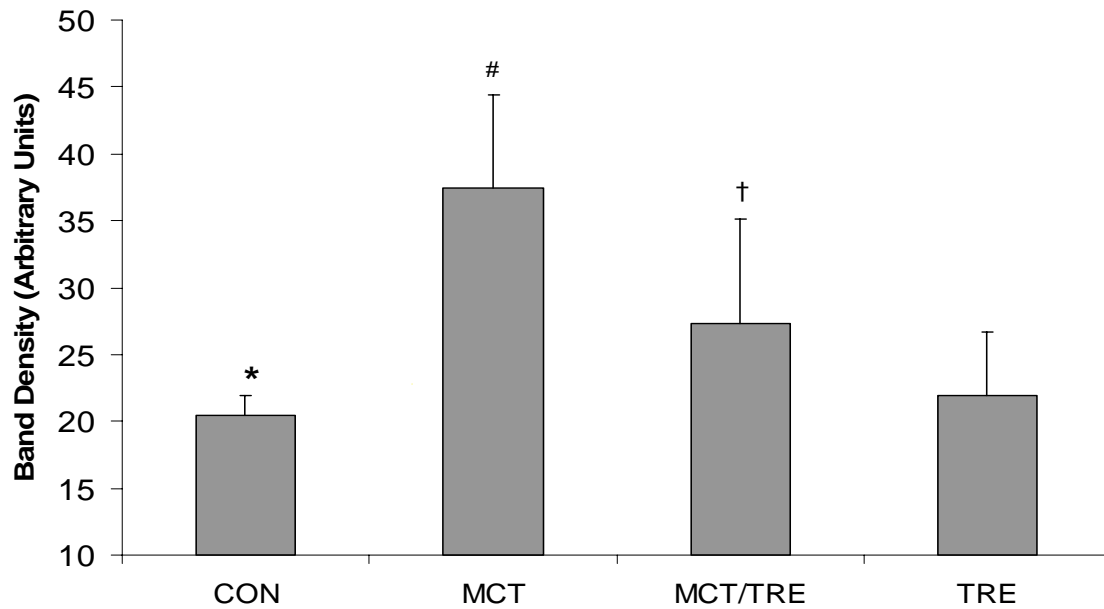


**Figure 9. PPAR- $\gamma$  levels decrease with treprostinil treatment in a rat model of pulmonary hypertension.** Figure 9a, two representative Western blots of PPAR- $\gamma$  (60 kDa). Figure 9b, quantitative analysis of PPAR- $\gamma$  protein bands visualized by Western blot (represented in figure 9a). MCT increased the protein levels of PPAR- $\gamma$  in rat whole lung homogenates. Lung homogenates of treprostinil-treated rats exhibited a significant reduction in PPAR- $\gamma$  protein levels. \* p=0.001 vs. MCT, # p=0.001 vs. TRE, † p=0.029 vs. MCT

9a



9b



## Discussion

The present study tested whether treprostinil treatment alters the hemodynamic changes and vascular remodeling associated with MCT-induced pulmonary hypertension. We found that treprostinil treatment was unable to abrogate elevations in mPAP and right ventricular hypertrophy associated with MCT. Likewise, treprostinil seemingly had no effect on vascular remodeling. Finally, we observed that treprostinil decreased PPAR- $\gamma$  protein expression in the lungs of MCT-exposed rats.

To our knowledge, this is the first rodent study, and only the second animal study (35; 51), to explore the effects of treprostinil *in vivo*, therefore, all findings should be considered novel. At the beginning of the experiment, we gave a one-time subcutaneous injection of MCT. Twenty-eight days later, MCT-exposed rats exhibited a significant increase in RVSP (Figure 2) and right ventricular hypertrophy (Figure 3) when compared to control animals. We also observed a positive correlation between RVSP and right ventricular hypertrophy, as measured by RV/(LV+septum) (Figure 4). Finally, we found that MCT rats developed a significant increase in MWT, as well as a reduction in lumen diameter in arteries with up to a 200  $\mu\text{m}$  external diameter (Figure 7). These results, which nearly replicate those seen in other animal studies of pulmonary hypertension (21; 23; 36; 45), led us to conclude that the rats used in these experiments suffered from chronic pulmonary hypertension related to MCT administration.

After establishing an animal model of pulmonary hypertension, we evaluated the effects of treprostinil on RVSP. MCT-exposed rats displayed significant increases in RVSP when compared to control rats. However, treprostinil treatment was unable to lessen increased RVSPs in rats that also received MCT (Figure 2). These results coincide

with human studies in which only small changes (~3 mm Hg), most of which were non-significant, in mPAP were seen after short-term treprostinil administration (50). Consequently, we increased the dose of treprostinil from 10 ng/kg/min to 150 ng/kg/min in an attempt to elicit a treprostinil response. The higher treprostinil dose still had no effect on MCT-induced elevations of RVSP. Additionally, although treprostinil-treated patients do not typically exhibit significant reductions in mPAP, they consistently show improvements in exercise hemodynamics such as exercise capacity (measured by the 6-minute walk test), signs and symptoms of pulmonary arterial hypertension, and the quality of life score (33; 43; 50). Unfortunately, although exercise hemodynamics can account for the observed clinical advancement in treprostinil-treated humans, these endpoints were not investigated in the present experiments, and therefore, could not be compared to human study results.

Next, we determined the effect of treprostinil on right ventricular hypertrophy (Figure 3). While MCT successfully induced right ventricular hypertrophy when compared to controls, continuous subcutaneous infusion of treprostinil was unable to lessen enlargement of the right ventricle. This finding opposes those seen in similar studies which found that MCT-induced right ventricular hypertrophy was attenuated with inhaled iloprost (49) and orally administered beraprost (38). We therefore hypothesized that treprostinil may not directly affect hemodynamic measurements, but instead, might primarily inhibit and/or reverse MCT-induced vascular remodeling and secondarily attenuate increases in RVSP and right ventricular hypertrophy.

Thus, we analyzed morphological changes in the pulmonary vasculature by two different methods. First, using a linear measurement model described by Geraci, et al.,

(14), we examined arteries of VVG-stained whole lung tissues. We found that MCT successfully increased MWT in vessels from  $<50\ \mu\text{m}$  to  $200\ \mu\text{m}$  and that treprostinil-treatment of MCT-exposed rats attenuated increased MWT in resistance vessels  $50\text{-}100\ \mu\text{m}$  in size (Figure 6). Although we used an established method of morphometrics, we found that we were limited in the number of vessels that could be measured since only vessels that were either perfectly or near perfectly cylindrical could be examined. Therefore, we resolved to reanalyze the same VVG-stained whole lung tissues utilizing ImagePro Plus®, a histological analysis software, to determine % MWT of each vessel. Using area measurements, we observed that treprostinil therapy did not significantly attenuate increases of % MWT in resistance (Figure 8) or conduit vessels. These results contradicted those initially found with the linear measurement morphometry method, which showed that treprostinil-treatment significantly reduced MCT-induced vascular remodeling in vessels  $50\text{-}100\ \mu\text{m}$  in size. The inability of the % MWT data, calculated by vessel area measurements, to replicate our initial morphometry results led us to conclude that we detected a false positive attenuation of MWT in our original linear measurement analyses. Hence, we found that area measurements of % MWT represent the morphometric data in its true form. Likewise, the inability of treprostinil to reduce vascular remodeling could possibly explain why neither low-dose nor high-dose treprostinil attenuated elevations of RVSP and right ventricular hypertrophy. It therefore appears as though treprostinil is an ineffective treatment for increased RVSP, right ventricular hypertrophy, and vascular remodeling associated with MCT-induced pulmonary hypertension. We speculate that these negative outcomes could be attributed to the nature of the drug delivery system rather than the animal model since studies have

shown that other PGI<sub>2</sub> analogs successfully attenuate MCT-induced pulmonary hypertension (27; 38; 49). Although subcutaneous delivery of treprostinil seems ideal because of its less invasive nature, in fact, it could be less effective than IV or inhaled methods of administration given that the drug is not delivered directly to the pulmonary vasculature.

Finally, we investigated the effects of treprostinil on PPAR- $\gamma$  protein levels in whole lung homogenates (Figure 9). We found that administration of MCT significantly increased PPAR- $\gamma$  levels in comparison to control values. These results contradict those found by Ameshima, et al. (2), who found that PPAR- $\gamma$  protein expression was decreased in whole lung tissue extracts from pulmonary hypertensive patients. Furthermore, they established that PPAR- $\gamma$  mRNA was significantly decreased in patients with severe pulmonary hypertension when compared with normal lung tissue or tissue from patients with emphysema. Conversely, our findings support those of Diep, et al. (11), who reported that PPAR- $\gamma$  is abundantly expressed in blood vessels, particularly resistance arteries, of spontaneously hypertensive rats, indicating that PPAR- $\gamma$  in the vasculature may play an important role in vascular changes during the development of hypertension. Next, we observed that treprostinil treatment significantly reduced MCT increases in PPAR- $\gamma$  protein levels. These results agree with the findings by Hauser, et al. (19), who demonstrated that PPAR- $\gamma$  protein levels are significantly reduced in adipose cells and fibroblasts treated with PPAR- $\gamma$  ligands due to degradation of the receptor via the ubiquitin-proteasome pathway. Their studies also revealed that significant decreases in PPAR- $\gamma$  protein levels occur when PPAR- $\gamma$  ligands bind to the PPAR- $\gamma$  receptor resulting in the loss of receptor functionality. Accordingly, once PPAR- $\gamma$  becomes bound by

treprostinil, we would expect PPAR- $\gamma$  protein levels to decrease, which was our observed result. Thus, although it warrants further investigation, the study by Hauser, et al., provides supporting evidence that treprostinil, and possibly PGI<sub>2</sub> in general, could either act as PPAR- $\gamma$  ligands themselves or possibly serve to activate other known PPAR- $\gamma$  ligands in the pulmonary vasculature.

In conclusion, we have demonstrated that (1) rats exhibit increased RVSP, right ventricular hypertrophy, and vascular remodeling 28-days after receiving a one-time subcutaneous dose of MCT; and (2) treprostinil treatment of rodents with MCT-induced pulmonary hypertension does not attenuate elevations in RVSP, right ventricular hypertrophy or vascular remodeling associated with MCT-induced pulmonary hypertension. We also found that (3) PPAR- $\gamma$  protein levels in whole lung are significantly lowered in MCT-induced pulmonary hypertensive rats treated with treprostinil. Although we have not yet established that PPAR- $\gamma$  is an important therapeutic target, we speculate that further investigation of its role in pulmonary hypertension could reveal a mechanism in which PGI<sub>2</sub> elicits its effects on the pulmonary vasculature. Finally, although it appears as though treprostinil does not act as a cure to MCT-induced pulmonary hypertension, we speculate that treprostinil could serve as a palliative treatment. Hence, future animal studies could assess the effects of treprostinil on more subtle positive outcomes such as exercise capacity and the physical dimension of quality of life.

## Reference List

1. **Ali S, Davis MG, Becker MW and Dorn GW.** Thromboxane A<sub>2</sub> stimulates vascular smooth muscle hypertrophy by up-regulating the synthesis and release of endogenous basic fibroblast growth factor. *J Biol Chem* 268: 17397-17403, 1993.
2. **Ameshima S, Golpon H, Cool CD, Chan D, Vandivier RW, Gardai SJ, Wick M, Nemenoff RA, Geraci MW and Voelkel NF.** Peroxisome proliferator-activated receptor gamma (PPARgamma) expression is decreased in pulmonary hypertension and affects endothelial cell growth. *Circ Res* 92: 1162-1169, 2003.
3. **Aranda M, Bradford KK and Pearl RG.** Combined therapy with inhaled nitric oxide and intravenous vasodilators during acute and chronic experimental pulmonary hypertension. *Anesth Analg* 89: 152-158, 1999.
4. **Barst RJ, Rubin LJ, Long WA, McGoon MD, Rich S, Badesch DB, Groves BM, Tapson VF, Bourge RC, Brundage BH.** A comparison of continuous intravenous epoprostenol (prostacyclin) with conventional therapy for primary pulmonary hypertension. The Primary Pulmonary Hypertension Study Group. *N Engl J Med* 334: 296-302, 1996.
5. **Bishop-Bailey D, Hla T and Warner TD.** Intimal smooth muscle cells as a target for peroxisome proliferator-activated receptor-gamma ligand therapy. *Circ Res* 91: 210-217, 2002.
6. **Blumberg FC, Lorenz C, Wolf K, Sandner P, Riegger GA and Pfeifer M.** Increased pulmonary prostacyclin synthesis in rats with chronic hypoxic pulmonary hypertension. *Cardio Res* 55(1):171-7, 2002.
7. **Chazova I, Loyd JE, Zhdanov VS, Newman JH, Belenkov Y and Meyrick B.** Pulmonary artery adventitial changes and venous involvement in primary pulmonary hypertension. *Am J Pathol* 146: 389-397, 1995.
8. **Christman BW, McPherson CD, Newman JH, King GA, Bernard GR, Groves BM and Loyd JE.** An imbalance between the excretion of thromboxane and prostacyclin metabolites in pulmonary hypertension. *N Engl J Med* 327: 70-75, 1992.

9. **Clapp LH, Finney P, Turcato S, Tran S, Rubin LJ and Tinker A.** Differential effects of stable prostacyclin analogs on smooth muscle proliferation and cyclic AMP generation in human pulmonary artery. *Am J Respir Cell Mol Biol* 26: 194-201, 2002.
10. **Cottrill CM, Johnson GL and Gillespie MN.** Echocardiographic detection of pulmonary hypertension in anesthetized rats. *Res Commun Chem Pathol Pharmacol* 60: 189-196, 1988.
11. **Diep QN and Schiffrin EL.** Increased expression of peroxisome proliferator-activated receptor- $\alpha$  and - $\gamma$  in blood vessels of spontaneously hypertensive rats. *Hypertension* 38: 249-254, 2001.
12. **Dorfmuller P, Perros F, Balabanian K and Humbert M.** Inflammation in pulmonary arterial hypertension. *Eur Respir J* 22: 358-363, 2003.
13. **Edwards J and Heath D.** A description of six grades of structural changes in the pulmonary arteries with special reference to congenital septal defects. *Circulation* 18: 533-547, 1958.
14. **Geraci MW, Gao B, Shepherd DC, Moore MD, Westcott JY, Fagan KA, Alger LA, Tudor RM and Voelkel NF.** Pulmonary prostacyclin synthase overexpression in transgenic mice protects against development of hypoxic pulmonary hypertension. *J Clin Invest* 103: 1509-1515, 1999.
15. **Giaid A and Saleh D.** Reduced expression of endothelial nitric oxide synthase in the lungs of patients with pulmonary hypertension. *N Engl J Med* 333: 214-221, 1995.
16. **Giaid A, Yanagisawa M, Langleben D, Michel RP, Levy R, Shennib H, Kimura S, Masaki T, Duguid WP and Stewart DJ.** Expression of endothelin-1 in the lungs of patients with pulmonary hypertension. *N Engl J Med* 328: 1732-1739, 1993.
17. **Hanasaki K, Nakano T and Arita H.** Receptor-mediated mitogenic effect of thromboxane A<sub>2</sub> in vascular smooth muscle cells. *Biochem Pharmacol* 40: 2535-2542, 1990.

18. **Hatae T, Wada M, Yokoyama C, Shimonishi M and Tanabe T.** Prostacyclin-dependent apoptosis mediated by PPAR delta. *J Biol Chem* 276: 46260-46267, 2001.
19. **Hauser S, Adelmant G, Sarraf P, Wright HM, Mueller E and Spiegelman BM.** Degradation of the peroxisome proliferator-activated receptor gamma is linked to ligand-dependent activation. *J Biol Chem* 275: 18527-18533, 2000.
20. **Highland KB, Strange C, Mazur J and Simpson KN.** Treatment of pulmonary arterial hypertension: a preliminary decision analysis. *Chest* 124: 2087-2092, 2003.
21. **Hill LL and Pearl RG.** Combined inhaled nitric oxide and inhaled prostacyclin during experimental chronic pulmonary hypertension. *J Appl Physiol* 86: 1160-1164, 1999.
22. **Hoeper MM, Schwarze M, Ehlerding S, Adler-Schuermeyer A, Spiekeroetter E, Niedermeyer J, Hamm M and Fabel H.** Long-term treatment of primary pulmonary hypertension with aerosolized iloprost, a prostacyclin analogue. *N Engl J Med* 342: 1866-1870, 2000.
23. **Hoshikawa Y, Voelkel NF, Gesell TL, Moore MD, Morris KG, Alger LA, Narumiya S and Geraci MW.** Prostacyclin receptor-dependent modulation of pulmonary vascular remodeling. *Am J Respir Crit Care Med* 164: 314-318, 2001.
24. **Humbert M, Morrell NW, Archer SL, Stenmark KR, MacLean MR, Lang IM, Christman BW, Weir EK, Eickelberg O, Voelkel NF and Rabinovitch M.** Cellular and molecular pathobiology of pulmonary arterial hypertension. *J Am Coll Cardiol* 43: 13S-24S, 2004.
25. **Iglarz M, Touyz RM, Amiri F, Lavoie MF, Diep QN and Schiffrin EL.** Effect of peroxisome proliferator-activated receptor-alpha and -gamma activators on vascular remodeling in endothelin-dependent hypertension. *Arterioscler Thromb Vasc Biol* 23: 45-51, 2003.
26. **Ilkiw R, Todorovich-Hunter L, Maruyama K, Shin J and Rabinovitch M.** SC-39026, a serine elastase inhibitor, prevents muscularization of peripheral arteries, suggesting a mechanism of monocrotaline-induced pulmonary hypertension in rats. *Circ Res* 64: 814-825, 1989.

27. **Itoh T, Nagaya N, Fujii T, Iwase T, Nakanishi N, Hamada K, Kangawa K and Kimura H.** A combination of oral sildenafil and beraprost ameliorates pulmonary hypertension in rats. *Am J Respir Crit Care Med* 169: 34-38, 2004.
28. **Jones DA, Benjamin CW and Linseman DA.** Activation of thromboxane and prostacyclin receptors elicits opposing effects on vascular smooth muscle cell growth and mitogen-activated protein kinase signaling cascades. *Mol Pharmacol* 48: 890-896, 1995.
29. **Komuro I, Kurihara H, Sugiyama T, Yoshizumi M, Takaku F and Yazaki Y.** Endothelin stimulates c-fos and c-myc expression and proliferation of vascular smooth muscle cells. *FEBS Lett* 238: 249-252, 1988.
30. **Lim H and Dey SK.** A novel pathway of prostacyclin signaling-hanging out with nuclear receptors. *Endocrinology* 143: 3207-3210, 2002.
31. **Marx N, Bourcier T, Sukhova GK, Libby P and Plutzky J.** PPARgamma activation in human endothelial cells increases plasminogen activator inhibitor type-1 expression: PPARgamma as a potential mediator in vascular disease. *Arterioscler Thromb Vasc Biol* 19: 546-551, 1999.
32. **Marx N, Schonbeck U, Lazar MA, Libby P and Plutzky J.** Peroxisome proliferator-activated receptor gamma activators inhibit gene expression and migration in human vascular smooth muscle cells. *Circ Res* 83: 1097-1103, 1998.
33. **McLaughlin VV, Gaine SP, Barst RJ, Oudiz RJ, Bourge RC, Frost A, Robbins IM, Tapson VF, McGoon MD, Badesch DB, Sigman J, Roscigno R, Blackburn SD, Arneson C, Rubin LJ and Rich S.** Efficacy and safety of treprostinil: an epoprostenol analog for primary pulmonary hypertension. *J Cardiovasc Pharmacol* 41: 293-299, 2003.
34. **McLaughlin VV, Genthner DE, Panella MM and Rich S.** Reduction in pulmonary vascular resistance with long-term epoprostenol (prostacyclin) therapy in primary pulmonary hypertension. *N Engl J Med* 338: 273-277, 1998.
35. **McNulty MJ, Sailstad JM and Steffen RP.** The pharmacokinetics and pharmacodynamics of the prostacyclin analog 15AU81 in the anesthetized beagle dog. *Prostaglandins Leukot Essent Fatty Acids* 48: 159-166, 1993.

36. **Meyrick B, Gamble W and Reid L.** Development of Crotalaria pulmonary hypertension: hemodynamic and structural study. *Am J Physiol* 239: H692-H702, 1980.
37. **Meyrick B and Reid L.** Hypoxia-induced structural changes in the media and adventitia of the rat hilar pulmonary artery and their regression. *Am J Pathol* 100: 151-178, 1980.
38. **Miyata M, Ueno Y, Sekine H, Ito O, Sakuma F, Koike H, Nishio S, Nishimaki T and Kasukawa R.** Protective effect of beraprost sodium, a stable prostacyclin analogue, in development of monocrotaline-induced pulmonary hypertension. *J Cardiovasc Pharmacol* 27: 20-26, 1996.
39. **Moncada S, Gryglewski R, Bunting S and Vane JR.** An enzyme isolated from arteries transforms prostaglandin endoperoxides to an unstable substance that inhibits platelet aggregation. *Nature* 263: 663-665, 1976.
40. **Narumiya S, Sugimoto Y and Ushikubi F.** Prostanoid receptors: structures, properties, and functions. *Physiol Rev* 79: 1193-1226, 1999.
41. **Numaguchi Y, Naruse K, Harada M, Osanai H, Mokuno S, Murase K, Matsui H, Toki Y, Ito T, Okumura K and Hayakawa T.** Prostacyclin synthase gene transfer accelerates reendothelialization and inhibits neointimal formation in rat carotid arteries after balloon injury. *Arterioscler Thromb Vasc Biol* 19: 727-733, 1999.
42. **Olschewski H, Walmrath D, Schermuly R, Ghofrani A, Grimminger F and Seeger W.** Aerosolized prostacyclin and iloprost in severe pulmonary hypertension. *Ann Intern Med* 124: 820-824, 1996.
43. **Oudiz RJ, Schilz RJ, Barst RJ, Galie N, Rich S, Rubin LJ and Simonneau G.** Treprostinil, a prostacyclin analogue, in pulmonary arterial hypertension associated with connective tissue disease. *Chest* 126: 420-427, 2004.
44. **Plutzky J.** Peroxisome proliferator-activated receptors in endothelial cell biology. *Curr Opin Lipidol* 12: 511-518, 2001.
45. **Rabinovitch M, Gamble W, Nadas AS, Miettinen OS and Reid L.** Rat pulmonary circulation after chronic hypoxia: hemodynamic and structural features. *Am J Physiol* 236: H818-H827, 1979.

46. **Rich S, Dantzker DR, Ayres SM, Bergofsky EH, Brundage BH, Detre KM, Fishman AP, Goldring RM, Groves BM and Koerner SK.** Primary pulmonary hypertension. A national prospective study. *Ann Intern Med* 107: 216-223, 1987.
47. **Rosenberg HC and Rabinovitch M.** Endothelial injury and vascular reactivity in monocrotaline pulmonary hypertension. *Am J Physiol* 255: H1484-H1491, 1988.
48. **Saji T, Ozawa Y, Ishikita T, Matsuura H and Matsuo N.** Short-term hemodynamic effect of a new oral PGI<sub>2</sub> analogue, beraprost, in primary and secondary pulmonary hypertension. *Am J Cardiol* 78: 244-247, 1996.
49. **Schermuly RT, Kreisselmeier KP, Ghofrani HA, Samidurai A, Pullamsetti S, Weissmann N, Schudt C, Ermert L, Seeger W and Grimminger F.** Antiremodeling effects of iloprost and the dual-selective phosphodiesterase 3/4 inhibitor tolafentrine in chronic experimental pulmonary hypertension. *Circ Res* 94: 1101-1108, 2004.
50. **Simonneau G, Barst RJ, Galie N, Naeije R, Rich S, Bourge RC, Keogh A, Oudiz R, Frost A, Blackburn SD, Crow JW and Rubin LJ.** Continuous subcutaneous infusion of treprostinil, a prostacyclin analogue, in patients with pulmonary arterial hypertension: a double-blind, randomized, placebo-controlled trial. *Am J Respir Crit Care Med* 165: 800-804, 2002.
51. **Steffen RP and de la MM.** The effects of I5AU8I, a chemically stable prostacyclin analog, on the cardiovascular and renin-angiotensin systems of anesthetized dogs. *Prostaglandins Leukot Essent Fatty Acids* 43: 277-286, 1991.
52. **Sulica R and Poon M.** Current medical treatment of pulmonary arterial hypertension. *Mt Sinai J Med* 71: 103-114, 2004.
53. **Tontonoz P, Nagy L, Alvarez JG, Thomazy VA and Evans RM.** PPAR $\gamma$  promotes monocyte/macrophage differentiation and uptake of oxidized LDL. *Cell* 93: 241-252, 1998.
54. **Tuder RM, Cool CD, Geraci MW, Wang J, Abman SH, Wright L, Badesch D and Voelkel NF.** Prostacyclin synthase expression is decreased in lungs from patients with severe pulmonary hypertension. *Am J Respir Crit Care Med* 159: 1925-1932, 1999.

55. **Ueno M, Miyauchi T, Sakai S, Goto K and Yamaguchi I.** Endothelin-A-receptor antagonist and oral prostacyclin analog are comparably effective in ameliorating pulmonary hypertension and right ventricular hypertrophy in rats. *J Cardiovasc Pharmacol* 36: S305-S310, 2000.
56. **Ueno M, Miyauchi T, Sakai S, Yamauchi-Kohno R, Goto K and Yamaguchi I.** A combination of oral endothelin-A receptor antagonist and oral prostacyclin analogue is superior to each drug alone in ameliorating pulmonary hypertension in rats. *J Am Coll Cardiol* 40: 175-181, 2002.
57. **Wade M, Baker FJ, Roscigno R, DellaMaestra W, Hunt TL and Lai AA.** Absolute bioavailability and pharmacokinetics of treprostinil sodium administered by acute subcutaneous infusion. *J Clin Pharmacol* 44: 83-88, 2004.
58. **Yanagisawa M, Kurihara H, Kimura S, Tomobe Y, Kobayashi M, Mitsui Y, Yazaki Y, Goto K and Masaki T.** A novel potent vasoconstrictor peptide produced by vascular endothelial cells. *Nature* 332: 411-415, 1988.

## VITA

Shena L. Latcham was born March 20, 1978 in Kansas City, Missouri. In 1996, she began attending college at the University of Missouri-Columbia. In December 2000, Shena received her Bachelor of Science degree in Biology. After graduation, she moved back to Kansas City where she began working as a laboratory technician in the Pulmonary and Infectious Diseases laboratory at the University of Missouri-Kansas City School of Medicine. In August 2002, Shena began graduate school in the Department of Medical Pharmacology and Physiology at the University of Missouri-Columbia. In May 2005, she earned her Master's of Science degree in Physiology.